

# The Cyclohexene Ring as Bioisostere of a Furanose Ring: Synthesis and Antiviral Activity of Cyclohexenyl Nucleosides

Piet Herdewijn<sup>a,\*</sup> and Erik De Clercq<sup>b</sup>

<sup>a</sup>Laboratory of Medicinal Chemistry, K.U. Leuven, Rega Institute for Medical Research, Minderbroedersstraat 10, B-3000 Leuven, Belgium

<sup>b</sup>Laboratory of Antiviral Chemotherapy, K.U. Leuven, Rega Institute for Medical Research, Minderbroedersstraat 10, B-3000 Leuven, Belgium

Received 6 December 2000; accepted 12 April 2001

**Abstract**—The application of the bioisosteric concept between a furanose ring and a cyclohexene ring in the nucleoside field has led to the discovery of new potent antiviral agents. © 2001 Published by Elsevier Science Ltd.

## Conformational Analysis of Cyclohexene Ring and of Cyclohexenyl Nucleosides: The Cyclohexene Ring as Bioisostere of a Furanose Ring

The cyclohexene ring is not a very common structural element in medicinal chemistry, which means that few drugs have a substituted cyclohexene ring as core structure. One of the reasons is that it is not easy to synthesize chiral substituted cyclohexenes in high enantiomeric excess and in bulk quantities. In contrast, the cyclohexene ring often occurs in natural compounds such as steroids, vitamin A, taxol, as components of ethereal oils such as limonene, and morphines. In the first examples, the cyclohexene ring is derived from isoprene chemistry while in the last example, the cyclohexene ring originates from L-tyrosine.

A cyclohexene ring has structural properties that distinguish this ring system from common six-membered rings such as cyclohexane, cyclohexadiene, and benzene, and that allow us to categorize the cyclohexene ring as a (bio)isostere of a saturated furanose ring. Indeed, the conformational behavior of a cyclohexene ring is similar to that of a saturated five-membered ring and this is caused by the presence of two sp<sup>2</sup>-hybridized carbon atoms in the cyclohexene ring which reduce ring flexibility. A cyclohexene ring mainly exists in the half-chair forms, which interconvert via the symmetrical boat form. The free energy barrier is about 5.6 kcal/mol (Fig.

1).<sup>1</sup> The energy difference between the half-chair forms and the planar intermediate form is much higher.

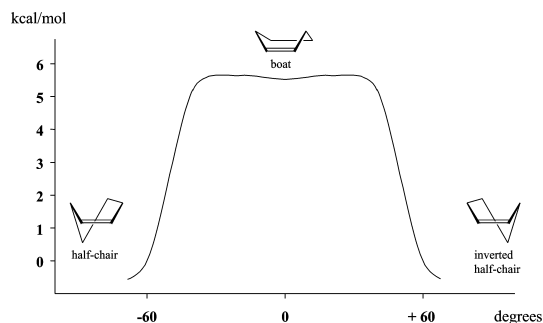


**Figure 1.** Energy profile for ring inversion in cyclohexene.<sup>1</sup>

In contrast to furanoses, where all possible ring forms are given by the two-dimensional pseudorotational cycle, the possible conformations of a six-membered ring are located on a three-dimensional conformational globe (Fig. 2).<sup>2,3</sup>

Each point on the globe represents one specific conformer and the energetically most favorable puckerings are located at the surface of the globe. The chair form and the inverted chair form are located at the poles of the globe (Fig. 2)<sup>4</sup> Each conformer on the surface of the globe can be defined by two puckering coordinates:  $\theta$  and  $\phi$  (Fig. 3). As an example, the equatorial plane represents the boat (B)–twist boat (TB) pseudorotational family for which  $\theta = 90^\circ$  and the  $\phi$  angle may have any value between  $0^\circ$  and  $360^\circ$  (pseudorotation is here a motion in the west–east direction) (Fig. 2). The

\*Corresponding author. Tel.: +32-1633-7387; fax: +32-1633-7340; e-mail: piet.herdewijn@rega.kuleuven.ac.be

half-boat (E)–half-chair (H) and the inverted half-boat–inverted half-chair pseudorotational cycles are situated approximately at the Tropic of Cancer on the northern hemisphere ( $\theta = 66.5^\circ$ ) and at the Tropic of Capricorn on the southern hemisphere ( $\theta = 113.5^\circ$ ) (Fig. 2).<sup>4</sup> It is clear that each form possesses an inverted form, located at antipodes of the globe and that there is a continuous change from *cis* to *trans* forms along a pseudorotational cycle. Ring interconversions, however, mostly take place on the surface of the globe (called semiversions). The planar form is the highest energy form and located at the center of the globe.

In contrast to cyclohexanes and cyclohexyl radicals, the introduction of a double bond into the cyclohexane ring limits the accessible conformational space (that can be populated by puckered ring conformers) to a plane (Fig. 2). This means that the conformational space of a cyclohexene ring is similar to that of a cyclopentane/furanose ring. As mentioned above, in cyclohexenes the half-chair forms are the global minimum and they interconvert via the boat transition states. The half-chair and inverted half-chair forms are located at  $\theta = 52.7^\circ$ ,  $\phi = 210^\circ$  and at  $\theta = 127.3^\circ$ ,  $\phi = 30^\circ$  on the conformational globe of cyclohexene (Fig. 2).

The boat and inverted boat forms are situated at  $\theta = 90^\circ$ ,  $\phi = 300^\circ$  and at  $\theta = 90^\circ$ ,  $\phi = 120^\circ$ . The ellipsis connecting the most stable conformers is moving along different pseudorotation itineraries. The  $C_2$  axis of the conformational energy surface of cyclohexene is shifted away of  $30^\circ$  (from the north–south axis) and is perpendicular to the ellipsis (Fig. 2). It is expected that most conformers of cyclohexene nucleosides at normal temperature are, likewise, locked in energy valleys along the ellipsis. Figure 4 explains the analogy between this

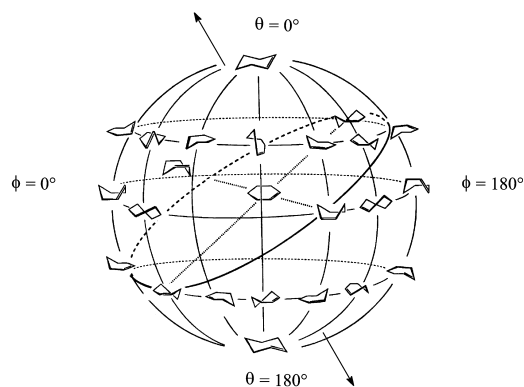


**Figure 2.** Conformational globe of cyclohexene. The ellipsis represents the most stable conformers of cyclohexene.<sup>4</sup>

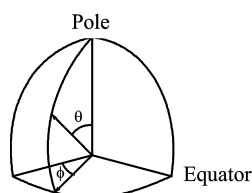


**Figure 3.** One octant of the sphere indicating  $\theta$  and  $\phi$  coordinates.<sup>2</sup>

ellipsis and the pseudorotational cycle of the furanose ring, which is the five-membered ring present in natural nucleosides. The  ${}^3_2T$  (north) and  ${}^2_3T$  (south) conformations of furanose find their structural equivalent in the  ${}^3_2H$  (north) and  ${}^2_3H$  (south) conformation of the cyclohexene ring (Fig. 4).

The boat and inverted boat forms of cyclohexenes then correspond with the O-4 envelope forms of the furanose ring (Fig. 4). The *N*- and *S*-type pseudorotamers of a furanose nucleoside convert into each other via the  $O_E$  pseudorotamer, because the  $O_E$  form has all substituents eclipsed and is of higher energy. For the same reason we can expect that the  ${}^3_2H$  and  ${}^2_3H$  conformers of cyclohexene nucleosides equilibrate via the  ${}^{1,4}B$  form. In the  ${}^{1,4}B$  form, all substituents are oriented pseudoaxially. When considering a (deoxy)cyclohexene nucleoside (e.g., **19**), we calculated by molecular mechanics that the energy difference between the  ${}^3_2H$  and  ${}^2_3H$  conformation of a cyclohexene nucleoside with an adenine base moiety is similar to the energy difference between the 3'-*endo* and the 2'-*endo* forms of a deoxyribose nucleoside and that the half-chair conformation with the base in a pseudoaxial position ( ${}^3_2H$ ) is preferred.<sup>5</sup> The energy difference of 1.6 kJ/mol corresponds to a ratio of about 7:3 of  ${}^3_2H$  versus the  ${}^2_3H$ . These data are in good agreement with the experimental values from NMR analysis. The conformation of a nucleoside is determined by competing steric and stereoelectronic effects. Considering cyclohexene nucleosides, an important stereoelectronic effect is the  $\pi \rightarrow \sigma^*_{C1-N}$  interaction between the C5'–C6' double bond and the heterocyclic aglycon. The  $\pi \rightarrow \sigma^*$

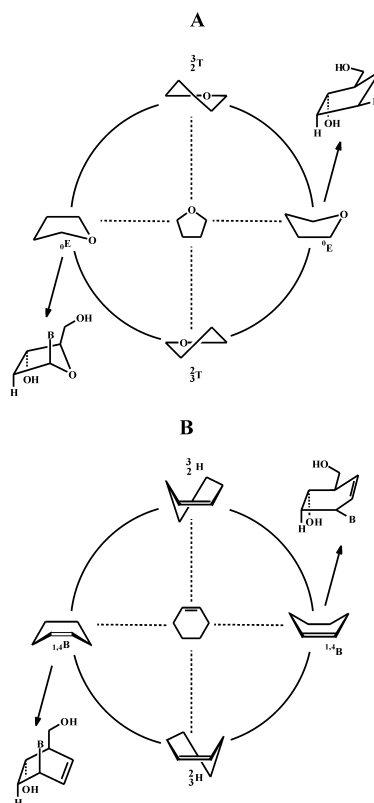


**Figure 4.** Relationship between pseudorotational cycle of (A) furanose and (B) cyclohexene.

effect can be explained as an overlap between the anti-bonding of C1'–N and the orbitals of the  $\pi$ -bond. It can be considered as the equivalent of the anomeric effect in furanose nucleosides (Fig. 5). In a 2'-deoxynucleoside, the anomeric effect favors the *N*-conformation while the gauche effect favors the *S*-conformation. In cyclohexene nucleosides, the anomeric effect is taken over by the  $\pi \rightarrow \sigma^*_{\text{C1'-N}}$  interactions, and favors the  $^3\text{H}$  conformation. Steric effects would favor the  $^3\text{H}$  conformation of cyclohexene nucleosides.

These opposing effects declare the conformational equilibrium of cyclohexenyl nucleosides which is very similar to the equilibria observed in furanose nucleosides. In cyclohexene nucleosides, the  $^3\text{H} \rightleftharpoons ^2\text{H}$  equilibrium is shifted towards the  $^3\text{H}$  conformation, in which the base moiety is pseudoaxially oriented (comparable with a ribofuranose nucleoside). Because of these considerations, we believed that cyclohexenyl nucleosides might have interesting biological properties.

### Synthesis of Cyclohexenyl Nucleosides

Cyclohexenyl nucleosides were synthesized starting from substituted cyclohexenes and the nucleobase was introduced by nucleophilic substitution including Mitsunobu reaction, by a gradual build up of the nucleobase, by a Michael-type addition reaction or by Pd(0) catalyzed substitution. The first synthesis of a cyclohexenyl nucleoside was described by Ramesh et al.<sup>6</sup> They synthesized several hydroxylated cyclohexenyl adenines, as potential inhibitors of *S*-adenosyl-homocysteine hydrolase, starting from 1,3-cyclohexadiene and *cis*-3,5-cyclohexadiene-1,2-diol (Scheme 1). Nucleophilic addition of adenine to 1,2-(isopropylidenedioxy)-5,6-epoxy-3-cyclohexene catalyzed by Pd(0) gave 9-[2-hydroxy-3,4-(isopropylidenedioxy)-5-cyclohexenyl]adenine in 90% yield. Deprotection of **1** with acid yielded the trihydroxycyclohexenyl adenine **2**. Compound **1** was converted in its deoxy derivative **3** and in 9-[3,4-dihydroxy-1-cyclohexenyl]adenine **4**.

Reaction of 1,2-(isopropylidenedioxy)-5,6-epoxy-3-cyclohexene with adenine and  $\text{K}_2\text{CO}_3$  (in the absence of Pd(0) catalyst), followed by deprotection with acid afforded **5** in 45% yield.

Reaction of adenine and 3,4-epoxycyclohexane with Pd(0) catalyst afforded 9-(4-hydroxy-2-cyclohexenyl)-adenine **6** in 35% yield (Scheme 2).  $\text{OsO}_4$  catalyzed dihydroxylation of **6**, followed by protection of the *cis*-diol function, elimination and deprotection, yielded 9-(2,3-dihydroxy-4-cyclohexenyl)adenine **7**.

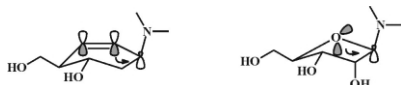
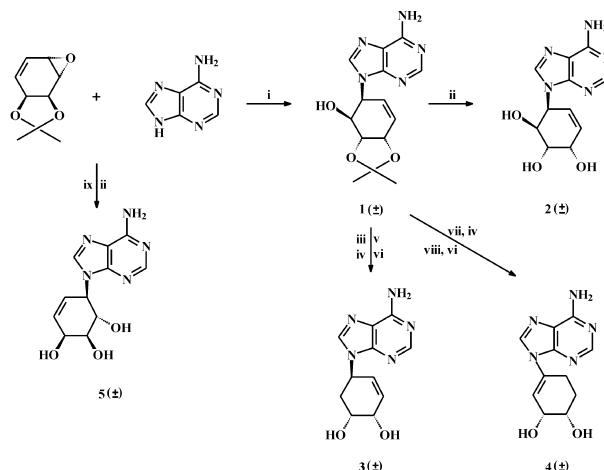


**Figure 5.** Comparison of the anomeric effect in furanose nucleosides with  $\pi \rightarrow \sigma^*_{\text{C1'-N}}$  effect in cyclohexene nucleosides.

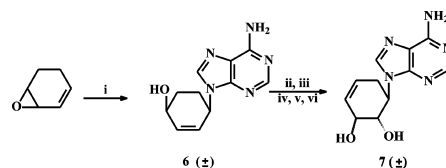
The inactivity of **2**, **3**, **4**, **5**, **6**, and **7** as inhibitors of bovine liver AdoHcy hydrolase, discouraged further research in this direction.

In the course of an anti-HIV program, Arango et al.<sup>7</sup> synthesized several cyclohexenyl thymine nucleosides (Scheme 3). Three reactions were investigated: (1) the  $\text{S}_{\text{N}}2$  substitution using thyminyl anion on chlorocyclohexenes and epoxycyclohexenes (leading to **8** and **9**); (2) the Pd(0) catalyzed addition of thymine to 3,4-epoxycyclohexene (leading to **10** and **11**); and (3) addition of nucleobases to methyl 1,3-cyclohexadien-1-carboxylate (leading to **12**). The last series of nucleoside analogues (type **12**) was synthesized both in the pyrimidine (T,C) and the purine series (A,G).<sup>8</sup> None of the compounds demonstrated anti-HIV activity.

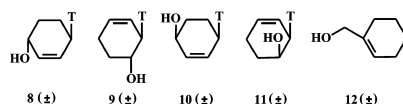
Phosphonate derivatives of cyclohexenyl nucleosides were synthesized starting from 1,4-*trans*-cyclohexenediol (Scheme 4).<sup>9</sup> The phosphonomethyl moiety was introduced after protection of one of both alcohol functions of **13**. Mitsunobu-type condensation reaction



**Scheme 1.** (i)  $[(i\text{-C}_3\text{H}_7\text{O})_3\text{P}]_4\text{Pd}$ , THF, DMSO, 90%; (ii) HCl, 87–90%; (iii) *N,N*-dimethylacetamide dimethyl acetal, MeOH, DMSO, 61–64%; (iv) BuLi, THF;  $\text{CS}_2$ ; MeI, 90%; (v)  $\text{Bu}_3\text{SnH}$ , AIBN, dioxane, 80%; (vi)  $\text{NH}_4\text{OH}$ , HCl, 68%; (vii)  $\text{PtO}_2/\text{H}_2$ , MeOH, 90%; (viii) DAST, DMAP,  $\text{CH}_2\text{Cl}_2$ , 95%; (ix)  $\text{K}_2\text{CO}_3$ , DMAC, 50%.



**Scheme 2.** (i)  $[(i\text{-C}_3\text{H}_7\text{O})_3\text{P}]_4\text{Pd}$ , adenine, THF, DMSO, 35%; (ii)  $\text{OsO}_4$ , NMO, acetone, 95%; (iii) DMP,  $\text{HClO}_4$ , acetone, 85%; (iv) *N,N*-dimethylacetamide dimethyl acetal, dioxane, 88%; (v) DAST,  $\text{CH}_2\text{Cl}_2$ , 90%; (vi)  $\text{NH}_4\text{OH}$ , HCl, 70%.

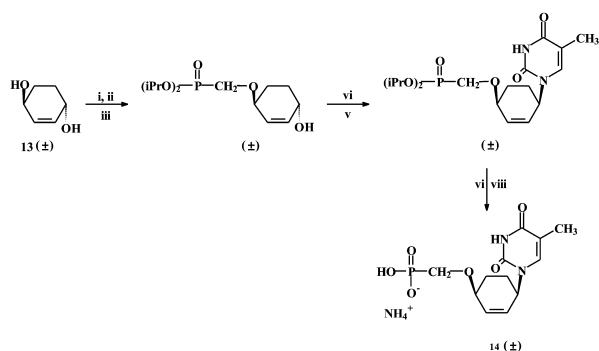


**Scheme 3.** Cyclohexenyl nucleosides synthesized in the course of an anti-HIV program.

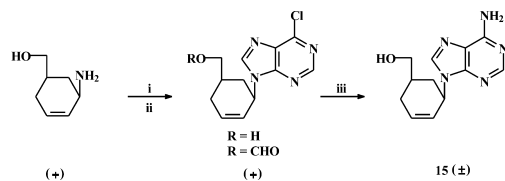
was used to introduce the nucleobases. The diisopropyl ester function of the phosphonate was hydrolyzed by reaction with trimethylsilyl bromide in DMF. All synthesized compounds (**14**, A, G, C, T bases) were inactive against herpes viruses and HIV.

5-Hydroxymethyl-2-cyclohexenyl nucleosides (**15**) were obtained by a gradual build up of the nucleobase from *cis*-(3-amino-4-cyclohexenyl) carbinol (Scheme 5).<sup>10</sup> The nucleosides (A, 9-azaA, G, 9-azaG) thus obtained exhibited no significant anti-HIV activity.

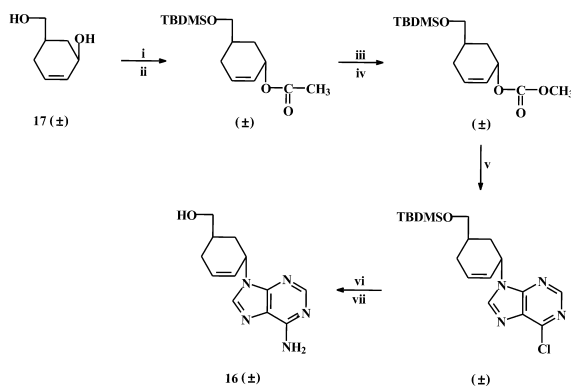
The *trans*-5-hydroxymethyl-2-cyclohexenyl nucleosides **16** were obtained from *cis*-3-hydroxy-4-cyclohexenyl-carbinol (Scheme 6).<sup>11</sup> The primary hydroxyl group of **17** was protected with a *tert*-butyldimethylsilyl group and the configuration of the carbon atom bearing the



**Scheme 4.** (i) TrCl, Et<sub>3</sub>N, DMAP, CH<sub>2</sub>Cl<sub>2</sub>; (ii) (iPrO)<sub>2</sub>POCH<sub>2</sub>OTs, NaH, DMF; (iii) 80% HOAc; (iv) *N*<sup>7</sup>-benzoylthymine, Ph<sub>3</sub>P, DEAD, dioxane; (v) MeOH, NH<sub>3</sub>; (vi) Me<sub>3</sub>SiBr, DMF; (vii) 10% Pd/C, H<sub>2</sub>, EtOH.



**Scheme 5.** (i) 5-amino-4,6-dichloropyrimidine, Et<sub>3</sub>N, BuOH, 83%; (ii) (EtO)<sub>3</sub>CH, HCl, DMF, 64%; (iii) NH<sub>3</sub>, MeOH, 77%.



**Scheme 6.** (i) TBDMSCl, Im, CH<sub>2</sub>Cl<sub>2</sub>, 44%; (ii) AcOH, Ph<sub>3</sub>P, DEAD, THF, 93%; (iii) K<sub>2</sub>CO<sub>3</sub>, MeOH, 93%; (iv) (MeOCO)<sub>2</sub>O, DMAP, THF, 78%; (v) 6-chloropurine, NaH, (Ph<sub>3</sub>P)<sub>4</sub>Pd, DMF, 30%; (vi) TBAF, THF, AcOH, 94%; (vii) NH<sub>3</sub>, MeOH, 100%.

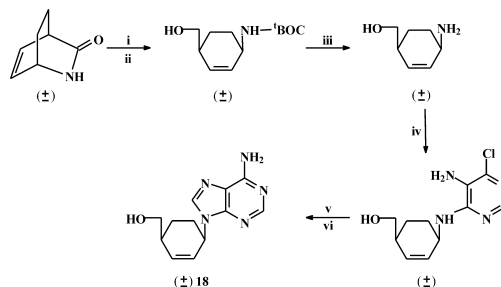
secondary hydroxyl group was inverted. Deprotection of the acetate and reaction with dimethylpyrocarbonate gave a carbonate that was used for coupling of the nucleobase. Reaction of the carbonate with 6-chloropurine under palladium coupling conditions, followed by desilylation and amination yielded *trans*-[3-(6-amino-9*H*-purin-9-yl)-4-cyclohexenyl]carbinol **16**. None of the synthesized compounds (A, G, and I) showed any activity against HSV-1 or HIV-1.

4-Hydroxymethyl-2-cyclohexenyl nucleosides **18** were synthesized by Katagiri et al. (Scheme 7)<sup>12</sup> and by Konkel and Vince (Scheme 8).<sup>13</sup> The first approach started from a bicycloamide and the amide bond of the bicycloamide was cleaved using NaBH<sub>4</sub> and the *t*-butoxycarbonyl group was removed with trifluoroacetic acid.<sup>12</sup> Purine ring construction yielded the desired nucleoside with adenine or guanine as the base moiety.

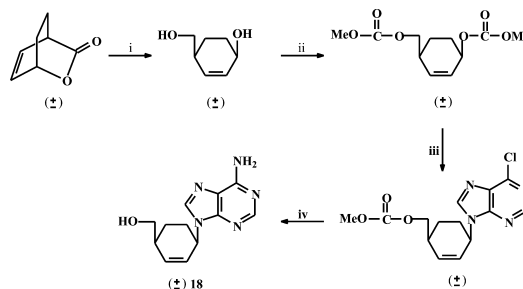
The method of Konkel and Vince started with 2-oxabicyclo[2.2.2]oct-5-en-3-one, which was reduced to *cis*-4-hydroxy-2-cyclohexenyl carbinol.<sup>13</sup>

Reactions of this diol with dimethylpyrocarbonate and coupling of the purine moiety using palladium resulted in the formation of the desired nucleosides.

All previous synthetic work was characterized by the fact that (a) all synthesized compounds were obtained as enantiomeric mixtures, and (b) all compounds were inactive in antiviral evaluation systems. However, two recent publications describe the first enantioselective synthesis of cyclohexenyl nucleosides and potent antiviral activity of cyclohexenyl G nucleosides (**19** and **20**).<sup>5,14</sup>



**Scheme 7.** (i) (tBOC)<sub>2</sub>O, Et<sub>3</sub>N, DMAP, 97%; (ii) NaBH<sub>4</sub>, MeOH, 98%; (iii) CF<sub>3</sub>COOH; (iv) 5-amino-4,6-dichloropyrimidine, DIEA, BuOH, 50%; (v) (EtO)<sub>3</sub>CH, HCl, 95%; (vi) NH<sub>3</sub>, MeOH, 74%.



**Scheme 8.** (i) LiAlH<sub>4</sub>, Et<sub>2</sub>O, 84%; (ii) (MeOCO)<sub>2</sub>O, DMAP, THF, 80%; (iii) 6-chloropurine, NaH, DMF, (Ph<sub>3</sub>P)<sub>4</sub>Pd, 57%; (iv) NH<sub>3</sub>, MeOH, 79%. No biological data are reported for these compounds.

The first enantiospecific synthesis of cyclohexenyl nucleosides used *R*-(-)-carvone as natural starting material,<sup>5,15</sup> which was first converted into 5-benzyloxy-3-(*tert*-butyldimethylsilyloxy)-2-methylenecyclohexanol in seven steps (Scheme 9). Hydroboration with 9-BBN afforded 5-benzyloxy-3-(*tert*-butyldimethylsilyloxy)-2-hydroxymethylene cyclohexanol in 74% yield.

The primary hydroxyl group was protected using TBDMSCl and the secondary alcohol group was mesylated. Hydrogenolytic cleavage using Pd/C and HCOONH<sub>4</sub> in MeOH, followed by oxidation of the alcohol function resulted in the direct isolation of the enone. Finally, the enone was reduced in a stereoselective way and the nucleobase introduced by Mitsunobu reaction.

The *L*-analogue<sup>14</sup> was obtained in a similar way but using another protected isomer of 2-hydroxymethyl-1,3,5-cyclohexanetriol as starting material (Scheme 10). The intermediate was converted to the dibenzoate. The

equatorial TBDMS group was selectively removed and the obtained alcohol was mesylated. After removing the other TBDMS group and oxidation of the resulting alcohol function, the desired enone was obtained. Stereoselective reduction followed by Mitsunobu reaction for introduction of base moiety and deprotection, yielded *L*-cyclohexenyl G.

### Antiviral Activity

D-Cyclohexenyl G and *L*-cyclohexenyl G were evaluated against a whole range of herpes viruses and their activity was compared with the activity of acyclovir and ganciclovir (Table 1).<sup>14,16</sup> A salient feature is that the antiviral potency and activity spectrum of both enantiomers were remarkably similar.

In comparison with acyclovir, the *D*- and *L*-cyclohexenyl guanines were slightly more potent against HSV-1 and slightly less potent against HSV-2. *D*- and *L*-Cyclohexenyl G were equipotent with acyclovir in inhibiting VZV replication. The virus-encoded thymidine kinase contributes to the activity of both compounds against HSV-1 and VZV, since they were less active against TK<sup>-</sup> than TK<sup>+</sup> HSV-1 or VZV-strains (the antiviral activity, however, was much greater than for acyclovir). *D*- and *L*-Cyclohexenyl G are the first examples of two enantiomeric nucleosides showing similar activity against a whole range of herpes viruses.

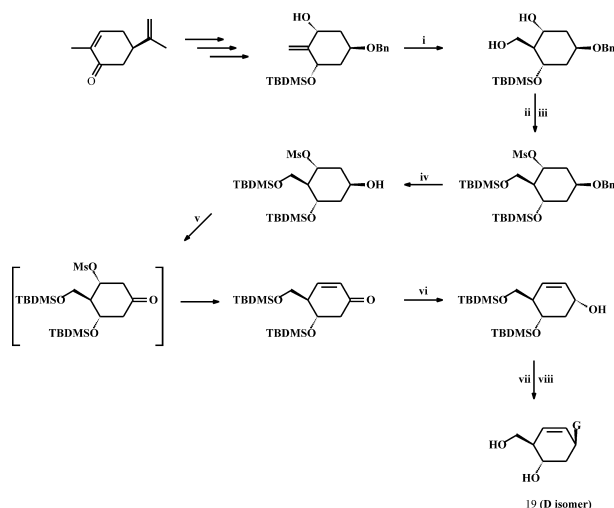
As intracellular phosphorylation in the virus-infected cells is supposed to be an important step in the enzymatic activation of cyclohexenyl G nucleoside, we carried out molecular modeling studies using *D*- and *L*-cyclohexenyl G and HSV-1 thymidine kinase as players. The main question that was asked is how enantiomeric nucleosides can be bound to the same enzyme.

We analyzed before that cyclohexenyl G preferentially occurs in the <sup>3</sup>H conformation with a pseudoaxial oriented base moiety (Fig. 5) and an anti-glycoside torsion angle. This conformation is more stable than the <sup>2</sup>H conformation with a pseudoequatorial base moiety.

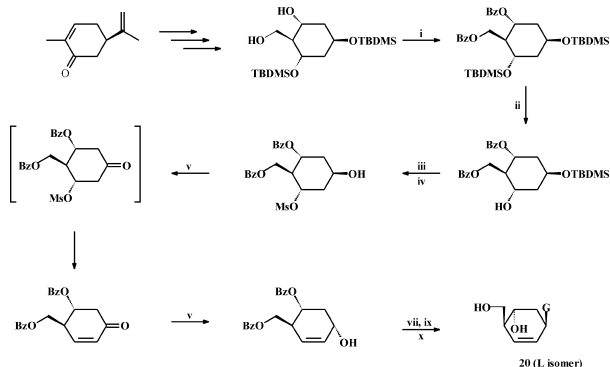
*D*- and *L*-Cyclohexenyl G were docked in the active site of the HSV-1 thymidine kinase with the guanine base moiety anchored to Gln-125 by double hydrogen bonds and the hydroxymethyl groups anchored to Arg-163 via hydrogen bonding (Fig. 6a and b).

These are the same contacts as found in the crystal structure of HSV-1 thymidine kinase complexed with penciclovir, which was used as starting model.

The compounds (*D*- and *L*-cyclohexenyl G) with the pseudoaxial oriented base moiety could not be accommodated in the active site due to difficulties of making contact between the primary hydroxy group of the nucleoside and Arg-163. However, the cyclohexenyl nucleosides can be nicely fit in the active site in their high energy conformation, that is with a pseudoequatorial oriented base moiety in the *syn* conformation. The



**Scheme 9.** (i) 9-BBN, THF and NaOH, EtOH, H<sub>2</sub>O<sub>2</sub>; (ii) TBDMSCl, Im, DMF, 70%; (iii) MsCl, Et<sub>3</sub>N, CH<sub>2</sub>Cl<sub>2</sub>, 92%; (iv) Pd/C; HCOONH<sub>4</sub>, MeOH, 97%; (v) MnO<sub>2</sub>, CH<sub>2</sub>Cl<sub>2</sub>, 40% (+ 53% starting material); (vi) NaBH<sub>4</sub>, CeCl<sub>3</sub>·7H<sub>2</sub>O, MeOH; (vii) 2-amino-6-chloropurine, DEAD, Ph<sub>3</sub>P, dioxane; (viii) CF<sub>3</sub>COOH, H<sub>2</sub>O, 46%.

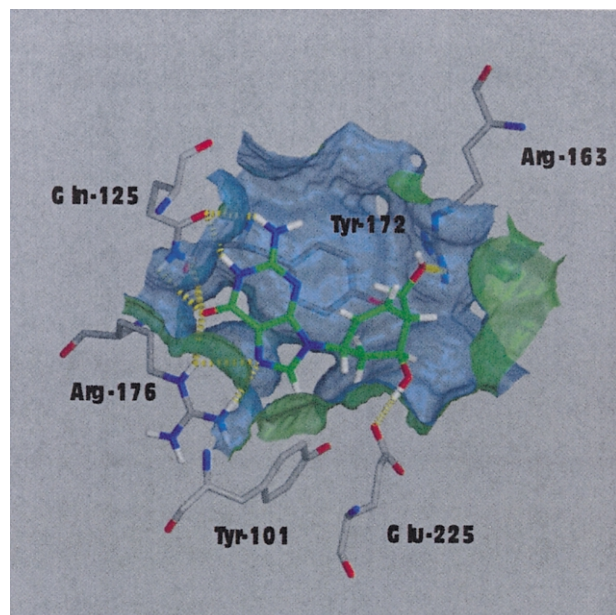


**Scheme 10.** (i) Bz<sub>2</sub>O, DMAP, CH<sub>2</sub>Cl<sub>2</sub>, 98%; (ii) TBAF, THF, 74%; (iii) MsCl, Et<sub>3</sub>N, CH<sub>2</sub>Cl<sub>2</sub>, 98%; (iv) TBAF, THF, 86%; (v) PDC, CH<sub>2</sub>Cl<sub>2</sub>, 68%; (vi) NaBH<sub>4</sub>, CeCl<sub>3</sub>·7H<sub>2</sub>O, MeOH, 75%; (vii) 2-amino-6-chloropurine, DEAD, Ph<sub>3</sub>P, dioxane; (ix) CF<sub>3</sub>COOH, H<sub>2</sub>O, 58%; (x) NH<sub>3</sub>, MeOH, 73%.

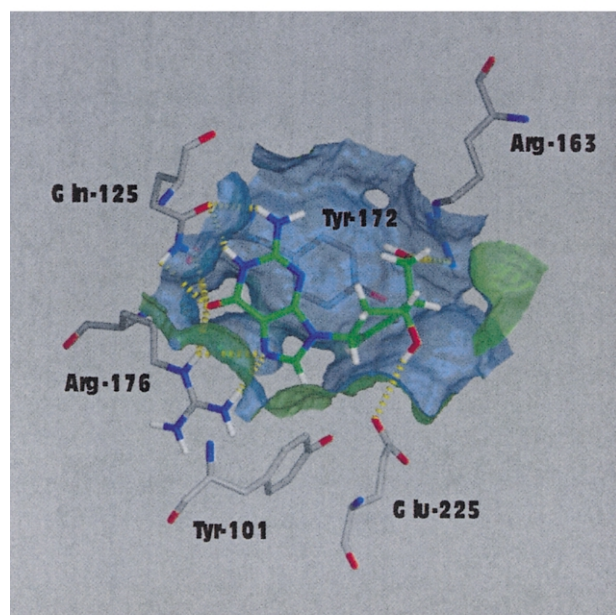
**Table 1.** Activity of D- and L-cyclohexenyl G against herpes viruses and against HBV (IC<sub>50</sub> µg/mL)

	D-Cyclohexenyl G	L-Cyclohexenyl G	Acyclovir	Ganciclovir
HSV-1 (KOS)	0.002	0.003	0.01	0.001
HSV-1 (TK <sup>-</sup> KOS)	0.38	1.28	9.6	0.48
HSV-2 (G)	0.05	0.07	0.02	0.002
VZV (YS)	0.49	1.2	1.1	ND
VZV (TK <sup>-</sup> KOS)	2.1	5.8	13	ND
HCMV (AD169)	0.6	1.5	ND	0.6
HBV (Hep AD79)			> 50	45

<sup>a</sup>Value for the racemice mixture of D- and L-cyclohexenyl G.



(a)



(b)

**Figure 6.** (a) Modeling of D-cyclohexenyl G in the active site of HSV-1 thymidine kinase. (b) Modeling of L-cyclohexenyl G in the active site of HSV-1 thymidine kinase.

guanine bases of D- and L-cyclohexenyl G are stacked against Tyr-172 and bound to Gln-125 via four hydrogen bonds. Likewise, Arg-176 is involved in hydrogen bond interactions with the guanine base, although the interaction with D-cyclohexenyl G (Fig. 6a) is somewhat stronger than with L-cyclohexenyl G (Fig. 6b). Similar observations are made for the hydrogen bonds between Glu-225 and the secondary alcohol function of the pseudosugar moiety.

The hydrogen bond with Glu-225 is 1.3 Å longer in the L-cyclohexenyl G than in the D-cyclohexenyl G complex. The primary hydroxyl groups are well associated to Arg-163 via one hydrogen bond. These observations are reflected in the calculated interaction energy between the cyclohexenyl G nucleosides and neighboring amino acid residues. A slight difference is noticed for both nucleosides, and the D-cyclohexenyl G/thymidine kinase complex is somewhat more stable than the L-cyclohexenyl G/thymidine kinase complex. This is mainly attributed to a difference in interaction energy between enzyme and the pseudosugar moiety, that is the secondary hydroxyl group of the cyclohexene ring and Glu-225 (and to a lesser extent between the primary hydroxyl group and Arg-163).

An interesting and unexpected conclusion is that the same amino acids are involved in binding the two enantiomeric nucleosides.

D- and L-Cyclohexenyl G show activity against HCMV at the same concentration as ganciclovir, and in addition, D- and L-cyclohexenyl G retained marked activity against HCMV strains that are resistant to ganciclovir (Table 2). As HCMV does not code for its own thymidine kinase, other phosphotransferases may be involved in the mechanism of action of cyclohexenyl nucleosides against HCMV. The activity spectrum of the cyclohexenyl G nucleosides goes beyond the herpes viruses, as the racemic mixture of cyclohexenyl G is about 10-fold more potent against hepatitis B virus (HBV) than penciclovir.<sup>16</sup>

## Conclusions

Conformational analysis of cyclohexenyl nucleosides has led to the conclusion that this sugar-modified nucleoside might be the best mimic of a natural furanose nucleoside. These nucleoside analogues were

**Table 2.** Activity of D- and L-cyclohexenyl G against various strains of HCMV (EC<sub>50</sub> µg/mL)

	D-Cyclohexenyl G	L-Cyclohexenyl G	Acyclovir	Ganciclovir
AD 169	0.47	1.05	16	0.77
Davis	0.83	3.97	16	0.62
Ly 9990	0.38	0.79	ND	7.5
U 9070	0.13	0.4	ND	10.8

synthesized in a stereospecific way starting from carvone. Antiviral evaluation confirmed our hypothesis and both enantiomeric nucleosides show broad-spectrum antiherpes virus and anti-HBV activity.

### Acknowledgements

The authors are very grateful to Matheus Froeyen and Eveline Lescrinier for the picture describing the interactions between viral TK and the cyclohexenyl nucleosides. We are indebted to Chantal Biernaux for excellent editorial assistance.

### References and Notes

1. Anet, F. A. L.; Freedberg, D. I.; Storer, J. W.; Houk, K. N. *J. Am. Chem. Soc.* **1992**, *114*, 10969.
2. Cremer, D.; Pople, J. A. *J. Am. Chem. Soc.* **1975**, *97*, 1354.
3. Pickett, H. M.; Strauss, H. L. *J. Am. Chem. Soc.* **1970**, *92*, 7281.
4. Cremer, D.; Szabo, K. J. In *Conformational Behavior of Six-Membered Rings*; Juaristi, E., Ed.; VCH: New York, 1995; pp 59–135.
5. Wang, J.; Herdewijn, P. *J. Org. Chem.* **1999**, *64*, 7820.
6. Ramesh, K.; Wolfe, M. S.; Lee, Y.; Vander Velde, D.; Borchardt, R. T. *J. Org. Chem.* **1992**, *57*, 5861.
7. Arango, J. H.; Geer, A.; Rodriguez, J.; Young, P. E.; Scheiner, P. *Nucleosides Nucleotides* **1993**, *12*, 773.
8. Maurinsh, Y.; Schraml, J.; De Winter, H.; Blaton, N.; Peeters, O.; Lescrinier, E.; Rozenski, J.; Van Aerschot, A.; De Clercq, E.; Busson, R.; Herdewijn, P. *J. Org. Chem.* **1997**, *62*, 2861.
9. Pérez-Pérez, M.-J.; Rozenski, J.; Busson, R.; Herdewijn, P. *J. Org. Chem.* **1995**, *60*, 1531.
10. Konkel, M. J.; Vince, R. *Nucleosides Nucleotides* **1995**, *14*, 2061.
11. Konkel, M. J.; Vince, R. *Tetrahedron* **1996**, *52*, 8969.
12. Katagiri, N.; Ito, Y.; Shiraishi, T.; Maruyama, T.; Sato, Y.; Kaneko, C. *Nucleosides Nucleotides* **1996**, *15*, 631.
13. Konkel, M. J.; Vince, R. *Tetrahedron* **1996**, *52*, 799.
14. Wang, J.; Froeyen, M.; Hendrix, C.; Andrei, G.; Snoeck, R.; De Clercq, E.; Herdewijn, P. *J. Med. Chem.* **2000**, *43*, 736.
15. Wang, J.; Busson, R.; Blaton, N.; Rozenski, J.; Herdewijn, P. *J. Org. Chem.* **1998**, *63*, 3051.
16. De Clercq, E.; Andrei, G.; Snoeck, R.; De Bolle, L.; Naesens, L.; Degréve, B.; Balzarini, J.; Zhang, Y.; Schols, D.; Leyssen, P.; Neyts, J. *Nucleosides Nucleotides Nucleic Acids* **2000**, in press.